

# Enhanced performance of a dye-sensitized solar cell with an electrodeposited-platinum counter electrode

Chang Ho Yoon<sup>a</sup>, R. Vittal<sup>a</sup>, Jiwon Lee<sup>b</sup>, Won-Seok Chae<sup>c</sup>, Kang-Jin Kim<sup>a,\*</sup>

<sup>a</sup> Department of Chemistry, Korea University, Seoul 136-713, South Korea

<sup>b</sup> Samsung SDI Co. Ltd., Gyeonggi-do 449-577, South Korea

<sup>c</sup> Department of Chemistry, Daejin University, Pocheon, Gyeonggi-do 487-711, South Korea

Received 4 September 2007; received in revised form 24 October 2007; accepted 29 October 2007

Available online 21 December 2007

## Abstract

A counter electrode was prepared for a dye-sensitized solar cell (DSSC) through electrochemical deposition of mesoporous platinum on fluorine-doped tin oxide glass in the presence of a structure-directing nonionic surfactant, octaethylene glycol monohexadecyl ether (C<sub>16</sub>EO<sub>8</sub>). The DSSC fabricated with the electrochemically deposited Pt (ED-Pt) counter electrode rendered a higher solar-to-electricity conversion efficiency of 7.6%, compared with approximately 6.4% of the cells fabricated with the sputter-deposited or most commonly-employed thermal deposited Pt counter electrodes. This enhanced efficiency is attributed to the higher short-circuit photocurrent arising from the increases in the active surface area and light reflection as well as the decrease in the sheet resistance of the ED-Pt film, relative to those of the Pt films prepared by the other two deposition methods. The sputter-deposited Pt film yielded almost the same photovoltaic characteristics as the thermal deposited Pt film. The Pt films were characterized by FE-SEM, AFM, cyclic voltammetry, chronoamperometry, electrochemical impedance spectroscopy, sheet resistance measurements, adhesion tests, and light reflection tests.

© 2007 Elsevier Ltd. All rights reserved.

**Keywords:** Electrodeposited-Pt counter electrode; Thermal and sputter depositions; Active surface area; Charge transfer resistance; Dye-sensitized solar cell

## 1. Introduction

High electrochemical activity of the counter electrode is an important requirement for enhanced performance of a dye-sensitized solar cell (DSSC). A thin layer of Pt is well established as the catalyst on the counter electrode substrate, usually a fluorine-doped tin oxide (FTO) conducting glass. When the counter electrode is only FTO glass without a Pt layer, the conversion efficiency of the pertinent cell is very low (0.1%) [1]. This indicates clearly that the function of the counter electrode depends essentially on the deposited Pt on the substrate. The role of Pt in the counter electrode of a DSSC is to catalyze the reduction of triiodide, I<sub>3</sub><sup>-</sup>, ions that are produced by the oxidation of iodide ions in the electrolyte by the oxidized dye. This catalysis is required to reduce the voltage loss due to charge-transfer overpotential at the counter electrode. The fast triiodide reduc-

tion kinetics on the Pt/FTO electrode leads to minimum energy loss. The light-reflecting character of the Pt is also desirable for increasing the light harvesting efficiency of the sensitizing dye.

Until now, platinized FTO glass has been the preferred combination for the counter electrode of a DSSC, due to the excellent catalytic activity of Pt for the reduction of I<sub>3</sub><sup>-</sup> ions and due to its light reflecting nature. The counter electrode is usually prepared by spreading a drop of hydrogen hexachloroplatinate (H<sub>2</sub>PtCl<sub>6</sub>) 2-propanol solution on a conducting glass substrate, followed by its annealing at 450 °C. The platinized counter electrode of a DSSC is also prepared by depositing Pt particles onto conducting glass by sputtering [2,3]. These two references also reported that a 2 nm-thick sputtered-Pt is sufficient to obtain a reasonable charge transfer resistance, one of the important parameters of a DSSC.

The counter electrodes prepared with carbon-based materials such as activated carbon [4], carbon nanotubes [5], hard carbon spherule [6], and acetylene-black spheres [7] were also used in DSSCs; however, such cells generally showed lesser efficiencies than that obtainable in the case of a DSSC with

\* Corresponding author. Tel.: +822 3290 3127; fax: +822 3290 3121.  
E-mail address: [kjkim@korea.ac.kr](mailto:kjkim@korea.ac.kr) (K.-J. Kim).

Pt counter electrode [8]. Recently, Murakami et al. employed carbon black as the counter electrode catalyst in a DSSC and achieved a remarkable light-to-energy conversion efficiency of 9.1% under  $100 \text{ mW cm}^{-2}$  [9]. Saito et al. [10] used chemically polymerized poly(3,4-ethylenedioxythiophene) on an ITO glass to prepare the counter electrode and obtained a conversion efficiency, comparable to that of a DSSC using a sputter-deposited Pt counter electrode. Furthermore, Biancardo et al. reported that a counter electrode prepared by spin-coating of poly(3,4-ethylenedioxythiophene):polystyrenesulphonate (PEDOT:PSS) had shown a similar  $\text{I}_3^-/\text{I}^-$  catalytic activity to that of a Pt counter electrode in a quasi-solid state dye-sensitized solar cell [11].

The usual FTO substrate was replaced by stainless steel, Ni and other plastic materials by Ma et al. [12], with Pt layer being used as the catalyst in all the cases. They found that stainless steel, nickel substrates and the plastic substrate, polyethylene naphthalate film coated with tin-doped indium oxide (ITO-PEN 110) were not only stable in the electrolyte, but also rendered efficiencies for their DSSCs that are comparable to that of a cell with a platinized FTO counter electrode. Wang et al. prepared a counter electrode for a DSSC by thermal decomposition of  $\text{H}_2\text{PtCl}_6$  on NiP-plated glass and the conversion efficiency of the pertinent cell increased by 33%, compared with that of a cell with a Pt/FTO counter electrode [13].

Considering the vast literature published on various components of DSSCs, it may be said that very few publications are made on their counter electrodes, and that there hardly exist reports on their electrochemical preparation. Though Papageorgiou et al. have deposited Pt electrochemically on conducting tin oxide glass, their focus in that report was only to prepare an iodine/triiodide reduction catalyst for aqueous and organic media and no photovoltaic properties of DSSCs were studied [14].

We present in this paper preparation of a platinum counter electrode for a DSSC by electrodepositing mesoporous Pt on a conducting substrate, using a nonionic surfactant, octaethylene glycol monohexadecyl ether ( $\text{C}_{16}\text{EO}_8$ ), and the greatly enhanced performance of the pertinent DSSC, with reference to those of cells fabricated using thermal and sputter-deposited Pt counter electrodes.  $\text{C}_{16}\text{EO}_8$  was selected for achieving a regular structure for the electrochemically deposited Pt; this is based on the fact that this nonionic surfactant forms liquid crystalline phase which can be used as a template for the production of mesoporous Pt. [15]. This enhanced performance of the DSSC with the electrodeposited-Pt counter electrode assumes its importance in view of the considerations that thermal deposition is not well-suited for flexible plastic electrodes due to high-temperature annealing, and that sputter deposition is not cost efficient due to its vacuum process. That is to say that metallic platinum can be obtained directly on flexible plastic substrates in the case of electrodeposition and heating process can thus be avoided, which is not possible for such substrates through thermal deposition, because in the thermal deposition heating at  $100^\circ\text{C}$  and then annealing at  $450^\circ\text{C}$  is required for the formation of metallic platinum from  $\text{H}_2\text{PtCl}_6\cdot\text{H}_2\text{O}$  on the substrate.

## 2. Experimental

### 2.1. Preparation of the counter electrodes

The electrochemical preparation of a Pt counter electrode ( $0.8 \text{ cm} \times 1.0 \text{ cm}$ ) for a DSSC was accomplished, using a potentiostat/galvanostat (PAR EG&G Model 273A), in a home-made three-electrode cell, assembled with a Pt coil counter electrode, an Ag/AgCl reference electrode, and an FTO conducting glass (Pilkington Co., TEC 7, approximately 80% visible transmittance) as the working electrode. The deposition solution consisted of 0.42 g of  $\text{C}_{16}\text{EO}_8$  (octaethylene glycol monohexadecyl ether), 0.3 ml of 8%  $\text{H}_2\text{PtCl}_6\cdot\text{H}_2\text{O}$ , and 0.5 ml of distilled water. Prior to coating, the FTO conducting glass plate of dimensions  $1.5 \text{ cm} \times 1.5 \text{ cm}$  was subjected to ultrasonic cleaning using water and then ethanol. The potentiostatic deposition of Pt film on the FTO substrate was carried out at a constant potential of  $-0.06 \text{ V}$  vs. Ag/AgCl for 900 s. The Pt-electrodeposited conducting glass was placed in distilled water for 2 h to remove any remaining  $\text{C}_{16}\text{EO}_8$ . This process was repeated three times, each time rinsing the substrate with water, to ensure the complete removal of the residual surfactant. The Pt-deposited FTO glass was dried at  $100^\circ\text{C}$  for 10 min and annealed at  $450^\circ\text{C}$  for 30 min in the air. The heating and annealing at far higher temperatures for a total of 40 min ensures the complete removal of the surfactant, because the melting point of the nonionic surfactant, octaethylene glycol monohexadecyl ether ( $\text{C}_{16}\text{EO}_8$ ), is  $43\text{--}44^\circ\text{C}$ .

For thermal deposition, a drop of 5 mM  $\text{H}_2\text{PtCl}_6\cdot\text{H}_2\text{O}$  in 2-propanol was placed on the FTO glass substrate, followed by its drying and then annealing at  $380^\circ\text{C}$  for 15 min. Sputter deposition of Pt was carried out at the rate of 7 nm/min for 30 s using Ar as the sputtering gas, employing a direct-current method with a Hitachi E-1030 ion sputter. All the Pt counter electrodes of the DSSCs used in this study had an area of  $0.8 \text{ cm} \times 1.0 \text{ cm}$ .

### 2.2. Preparation of the photoanode and fabrication of the DSSC

$\text{TiO}_2$  photoanode was prepared as follows. A thin layer of non-porous  $\text{TiO}_2$  was deposited on a cleaned FTO glass from 5% Ti(IV) butoxide in ethanol by spin coating at 3000 rpm, followed by its annealing at  $450^\circ\text{C}$ . A porous  $\text{TiO}_2$  film of  $10 \mu\text{m}$  thickness was formed on this coated substrate by a doctor blade technique as follows. Ti-Nanoxide D paste was placed in a container and stirred for 2 h. From this stirred paste a  $\text{TiO}_2$  film was made on the above pretreated FTO glass, using the doctor blade technique. The film was dried at  $70^\circ\text{C}$  for 10 min before removing the tape used for fixing the thickness of the film, and then annealed at  $450^\circ\text{C}$  for 30 min. The resulting  $\text{TiO}_2$  film was sensitized with N719 dye by immersing it for 24 h in 0.3 mM ethanolic solution of the N719 dye ( $\text{Ru(II)L}_2(\text{NCS})_2\cdot 2\text{TBA}$ , where L = 2,2'-bipyridyl-4,4'-dicarboxylic acid). A 2-electrode sandwiched DSSC was fabricated according to the procedure given elsewhere [16]. The  $\text{TiO}_2$  photoanode had an active area of  $0.4 \text{ cm} \times 0.4 \text{ cm}$ . The electrolyte consisted of 0.05 M  $\text{I}_2$ , 0.1 M LiI, 0.6 M 1,2-dimethyl-3-hexylimidazolium iodide, and 0.5 M 4-*tert*-butylpyridine in 3-methoxypropionitrile.

### 2.3. Characterization of the Pt films and the DSSCs

A Hitachi S-4300 field emission-scanning electron microscope (SEM) was used to obtain the surface microstructure of mesoporous Pt, deposited by different techniques, as well as to obtain the thickness of the TiO<sub>2</sub> film. Atomic force microscopy (AFM, model: XW-100, PSI Co.) was used to obtain two-dimensional micrographs of the Pt-coated films, for an area of 5 μm × 5 μm in each case. The quantitative values of the root-mean-square roughness ( $R_{\text{rms}}$ ) of the films were obtained by using the built-in software of the AFM apparatus. Sheet resistances of the counter electrodes were measured by the four-point method using a model CMT-SR1000N of Chang Min Co., Korea. For measurement of light reflection of the Pt film, a light from the light source, model 95 ion laser of Lexcel Co was made incident to the film at an angle of 45°. The adhesion of the Pt film on the FTO substrate was tested according to the standard tape test (ASTM D 3359, cross-cut tape test).

Cyclic voltammograms were obtained in the electrolyte solution, containing 1 mM I<sub>2</sub>, 10 mM LiI, and 0.1 M LiClO<sub>4</sub> in acetonitrile, at a scan rate of 100 mV s<sup>-1</sup>, using an EG&G PARC 263A potentiostat. The electrochemical cell consisted of Pt working electrode (0.8 cm × 1.0 cm), prepared by thermal, sputter or electrochemical depositions, a Pt-wire auxiliary electrode and an Ag/AgCl reference electrode. Chronoamperometric curves with the Pt films, prepared by thermal, sputter and electrochemical depositions, were obtained with an EG&G PARC 263A potentiostat, using an electrochemical cell consisting of the Pt-film working electrode (0.8 cm × 1.0 cm), a Pt-wire auxiliary electrode and an Ag/AgCl reference electrode. Hundred millimolars of LiI was used as the electrolyte for the DSSC, whereas 10 mM of LiI was used as the electrolyte for electrochemical measurements. Sufficiently higher content of I<sub>2</sub> is required for a DSSC to sustain the reduction and oxidation reactions of triiodide and iodide species at the counter electrode and photoanode, respectively, for higher performance of the cell. For electrochemical studies 10 mM of LiI was sufficient. The presence of LiClO<sub>4</sub> ensures suppression of the electrostatic migration of electroactive species in the electrochemical cell, which is absent in a DSSC.

All chemicals were of analytical grade and used without further purification. All solutions were prepared using Milli Q (18.2 MΩ cm) H<sub>2</sub>O. Octaethylene glycol mono-hexadecyl ether (C<sub>16</sub>EO<sub>8</sub>, 98% pure), and 3-methoxypropionitrile (C<sub>4</sub>H<sub>7</sub>NO, 99% pure) were purchased from Fluka. Ti-Nanoxide D paste (TiO<sub>2</sub>), N719 dye were purchased from Solaronix SA and their assay was not available. Ti(IV) butoxide (97% pure), hydrogen hexachloroplatinate (IV) hydrate (H<sub>2</sub>PtCl<sub>6</sub>·H<sub>2</sub>O), iodine, lithium iodide (LiI), 4-*tert*-butylpyridine, and 2-propanol are more than 99% pure and purchased from Aldrich. Lithium perchlorate (LiClO<sub>4</sub>, 95%) was also purchased from Aldrich. Anhydrous ethanol was 99.9% pure and obtained from Carlo Erba and acetonitrile was from Junsei and 99.5% pure. 1,2-dimethyl-3-hexylimidazolium iodide (C<sub>11</sub>H<sub>21</sub>N<sub>2</sub>I) was obtained from C-TRI and was 98% pure.

Photocurrent density–voltage ( $J$ – $V$ ) curves of the DSSCs fabricated with different Pt counter electrodes were obtained using a Keithley M236 source measure unit. A 300 W Xe arc lamp (Oriol) with an AM 1.5 solar simulating filter for spectral correction served as the light source, and its light intensity was adjusted to 100 mW cm<sup>-2</sup> by using a Si solar cell. To complement the photocurrent behavior of the DSSCs, electrochemical impedance spectra were recorded over a frequency range of 0.05–10<sup>5</sup> Hz with an AC amplitude of 5 mV using an EG&G PARC 273A potentiostat with an M1025 frequency–response detector.

## 3. Results and discussion

### 3.1. Characterization of the Pt films

The Pt films prepared by the three deposition methods were characterized by FE-SEM, AFM, cyclic voltammetry, and chronoamperometry. Fig. 1a, b, and c show plane view FE-SEM images of the Pt films deposited on the FTO glasses by thermal, sputter, and electrochemical deposition methods, respectively. Both the thermal deposited (TD) and sputter-deposited (SD) Pt films show scale-like structures with granules. The TD platinum film has granules of imprecise boundaries in a nebulous environment, whereas the SD platinum film has well-defined

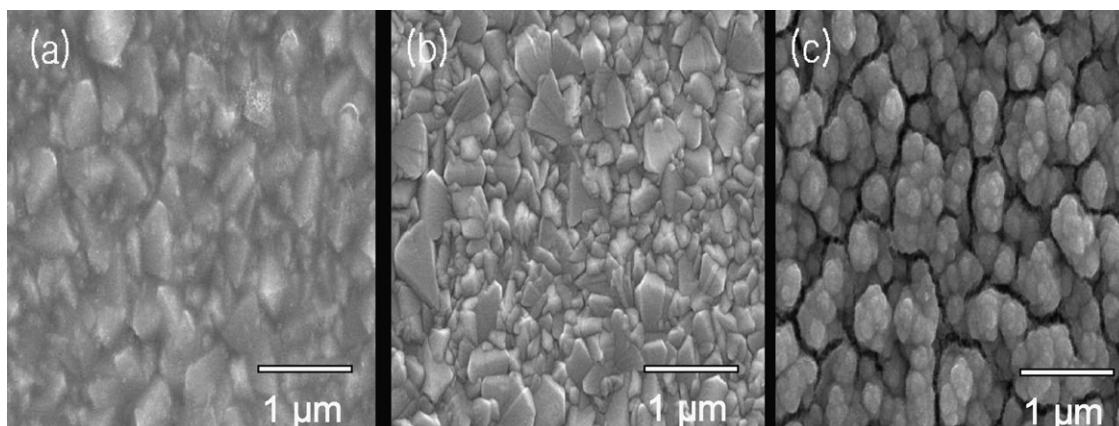


Fig. 1. FE-SEM images of the Pt films deposited by (a) thermal, (b) sputtering, and (c) electrochemical techniques on FTO substrates.

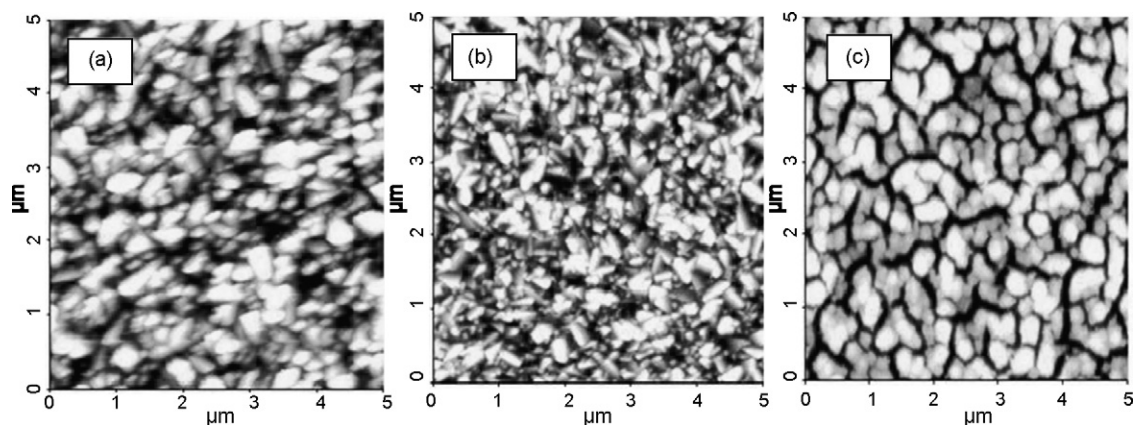


Fig. 2. Two-dimensional AFM surface images of the  $5\ \mu\text{m} \times 5\ \mu\text{m}$  Pt films deposited by (a) thermal, (b) sputtering, and (c) electrochemical methods on FTO substrates.

polyhedrons. Interestingly, the ED platinum shows spherical or elliptical granules and their clusters. Furthermore, the morphology of the ED film shows a robust mesostructure with accessible pores. The pattern of pores in the ED film is also periodically repeating. We believe that this regular structure in the ED film is effectively a cast of the structure of the liquid crystal phase formed in the electrochemical deposition process of Pt, because  $\text{C}_{16}\text{EO}_8$  was employed as a liquid crystal templating agent for metal depositions for ordered mesoporosity and for increasing the surface area of the deposited films [15,17]. A comparison among the three Pt films clearly shows that the ED-Pt film is more porous than the TD-Pt and SD-Pt films.

AFM topographic images of the TD-Pt, SD-Pt, and ED-Pt films are shown in Fig. 2, which gives additional evidence for the morphology of the films. The increased porosity of the ED-Pt film compared with those of the TD-Pt and SD-Pt films can be seen in the figure. The agglomerates in the ED film are of about  $0.3\text{--}0.5\ \mu\text{m}$ , while their size distribution in the cases of the TD-Pt and SD-Pt films can not be made with certain approximation, because of uncertain boundaries and irregular shapes of granules associated with them. The  $R_{\text{rms}}$  values of the Pt films were measured in order to identify the degree of the surface roughness of the films and are shown in Table 1. The ED-Pt film shows the largest  $R_{\text{rms}}$  value, approximately  $43\ \text{nm}$  over a  $5\ \mu\text{m} \times 5\ \mu\text{m}$  area of the film, implying that the ED-Pt film possesses the largest surface area among the three Pt films, in agreement with the results of the AFM topographic images. The  $R_{\text{rms}}$  values in Table 1 include the contribution from the FTO substrates. Nevertheless, the values indicate qualitatively the rel-

ative roughness of the very thin films of less than  $10\ \text{nm}$  in all the cases. As the amount of the associated platinum material ( $\sim 5\text{--}10\ \mu\text{g}/\text{cm}^2$ ) was insufficient for BET analysis, we could not determine the specific surface areas of the platinum films.

The relative active surface areas of the Pt films were verified by cyclic voltammetry and chronoamperometry from the rates of the oxidation of iodide and the reduction of iodine. Fig. 3 shows the cyclic voltammograms of the Pt films in the electrolyte solution, containing  $10\ \text{mM LiI}$ ,  $1\ \text{mM I}_2$ , and  $0.1\ \text{M LiClO}_4$  in acetonitrile. The CVs were obtained at the scan rate of  $100\ \text{mV s}^{-1}$ , using a cell assembled with the Pt working electrodes prepared by the three deposition methods, a Pt-wire auxiliary electrode and an Ag/AgCl reference electrode. The anodic peaks are denoted by I and II and the primes indicate the respective cathodic peaks. In an anodic sweep, iodide is oxidized sequentially to triiodide (peak I) and then to iodine (peak II) according to the reactions (1) and (2), respectively [18].

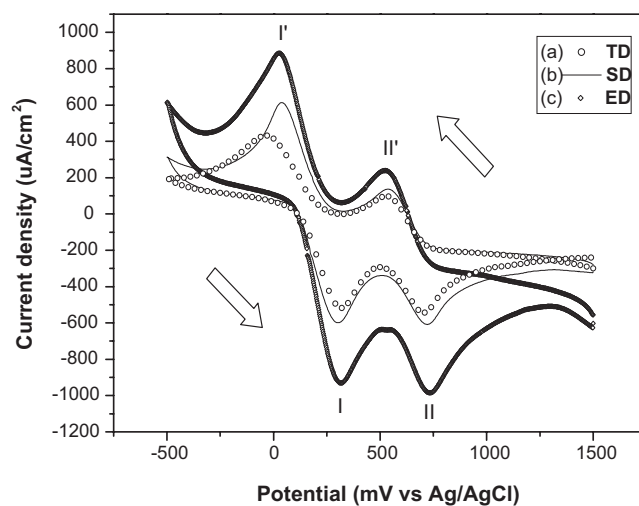
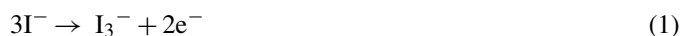


Fig. 3. Cyclic voltammograms with the TD, SD, and ED Pt films, obtained in the electrolyte containing  $1\ \text{mM I}_2$ ,  $10\ \text{mM LiI}$ , and  $0.1\ \text{M LiClO}_4$  in acetonitrile, at a scan rate of  $100\ \text{mV s}^{-1}$ .

Table 1

Root-mean-square roughness ( $R_{\text{rms}}$ ), reflectivity and sheet resistance of the Pt films prepared by thermal (TD), sputter (SD), and electrochemical (ED) depositions

Deposition method	$R_{\text{rms}}$ (nm)	Reflectivity at			Sheet resistance ( $\Omega/\text{sq}$ )
		488 nm	633 nm	830 nm	
TD	27	0.076	0.046	0.097	7.69
SD	28	0.18	0.20	0.35	7.46
ED	43	0.25	0.27	0.47	4.80

When the potential scan is reversed, iodine is reduced first to triiodide (peak II'), then to iodide (peak I'). Fig. 3 clearly reveals larger anodic and cathodic peaks and associated charges for the ED-Pt film than those for the TD-Pt and SD-Pt films. The increased peak heights and areas (or equivalent charges) for the ED-Pt film can be interpreted in terms of increased active surface area of this film [19] and in terms of enhanced reduction of  $I_3^-$  and oxidation of  $I^-$  at the ED-Pt working electrode, relative to those at the film electrodes obtained by the other deposition methods. Apparently, both of the reactions were facilitated by the highly accessible pore structure of the ED-Pt film through which the diffusions of  $I_3^-$  and  $I^-$  ions can be more rapid and less hindered than those in the TD-Pt and SD-Pt films. The increased active surface area of the ED-Pt film is also in tune with its porous structure as has been observed in its AFM image. This increased active surface area of ED-Pt film is desirable for DSSCs, because of the fact that reduction of  $I_3^-$  at the counter electrode in a DSSC entails larger active surface area.

The increased active surface area of the ED-Pt film deduced from the cyclic voltammograms is further verified by the chronoamperometric plots shown in Fig. 4. Each plot was obtained in an acetonitrile solution, containing 1 mM  $I_2$ , 10 mM LiI, and 0.1 M  $LiClO_4$  by using a Pt working electrode prepared by one of the deposition methods, a Pt-wire auxiliary electrode, and an Ag/AgCl reference electrode. The ED-Pt working electrode indeed showed the largest reduction current for  $I_3^-$  reduction and the largest oxidation current for  $I^-$  oxidation among the three Pt working electrodes, though the shapes of the  $I_3^-$  reduction plots are somewhat different from each other, probably due to the differences in the Pt film surface conditions.

The high active surface area arising from a tailored nanoporous nature of the ED-Pt film is advantageous for the performance of a DSSC, because the catalytic activity depends on the surface area of the catalyst, here the Pt film [14,19–21]. This is favorable for the reduction of  $I_3^-$  at the counter electrode,

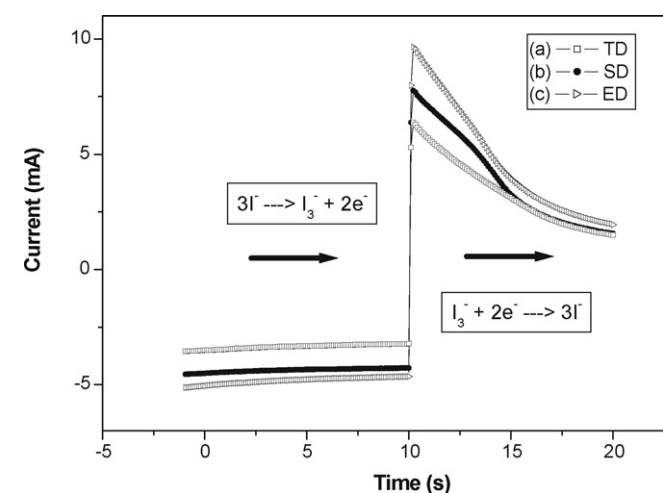


Fig. 4. Chronoamperometric curves with the Pt films in the electrolyte containing 10 mM LiI, 1 mM  $I_2$ , and 0.1 M  $LiClO_4$  in acetonitrile. The curves were obtained using the Pt working electrodes prepared by (a) thermal, (b) sputter, and (c) electrochemical depositions.

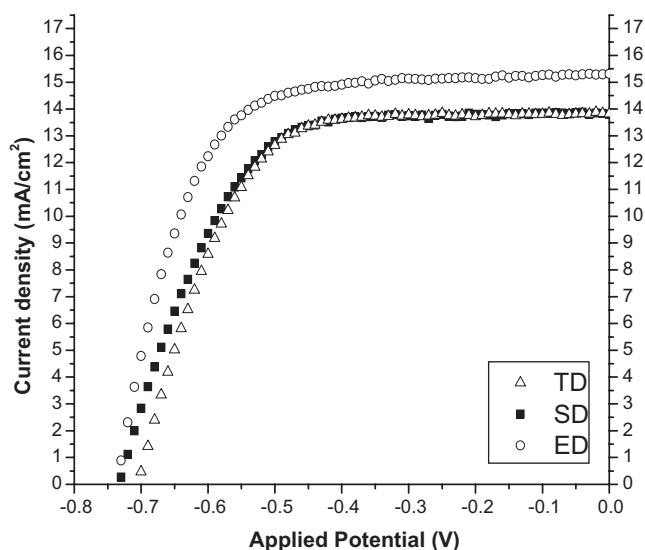


Fig. 5.  $J$ - $V$  curves of the DSSCs with the counter electrodes with TD-Pt, SD-Pt, and ED-Pt layers.

which in turn enhances the  $J_{sc}$  of a DSSC. We have measured average sheet resistances of the three Pt films along with that of a bare FTO glass substrate (Table 1). Surprisingly, the average sheet resistance of the ED-Pt film is found to be far less than those of the bare FTO glass (7.94  $\Omega$ /sq, not shown in the table) and the films of TD-Pt and SD-Pt. This lowest sheet resistance of the ED-Pt film may be attributed to its larger surface area, as a result of the more porous structure, and probably to its strong adhesion to the FTO substrate. To confirm the adhesion factor, the Pt films were subjected to the standard adhesion test (ASTM D 3359). The test revealed that the ED-Pt film adheres strongly to its FTO substrate. We are not certain to make a comparative statement with regard to the adhesion of the Pt films deposited by the three methods, because the films were too thin on the rough surface of the FTO glass plate to be able to differentiate their adhesion strengths.

### 3.2. $J$ - $V$ curves of the DSSCs

Fig. 5 shows the  $J$ - $V$  curves of the DSSCs with the TD-Pt, SD-Pt, and ED-Pt counter electrodes. The photovoltaic parameters are listed in Table 2. The short circuit photocurrent density ( $J_{sc}$ ) and the open-circuit voltage ( $V_{oc}$ ) of the DSSC with the ED-Pt counter electrode with a deposition time of 900 s are 15.38  $mA\ cm^{-2}$  and 0.73 V, compared with the  $J_{sc}$  of 13.87  $mA\ cm^{-2}$  and  $V_{oc}$  of 0.70 V of the cell with a TD-Pt counter electrode. Promoted by this increase in the  $J_{sc}$  and  $V_{oc}$  and an increase in the fill factor, the DSSC with the ED-

Table 2  
Photovoltaic parameters of the DSSCs with the counter electrodes with TD-Pt, SD-Pt, and ED-Pt layers

Deposition	$J_{sc}$ ( $mA\ cm^{-2}$ )	$V_{oc}$ (V)	FF	$\eta$ (%)
TD	13.87	0.70	0.63	6.3
SD	13.95	0.73	0.65	6.4
ED	15.38	0.73	0.68	7.6

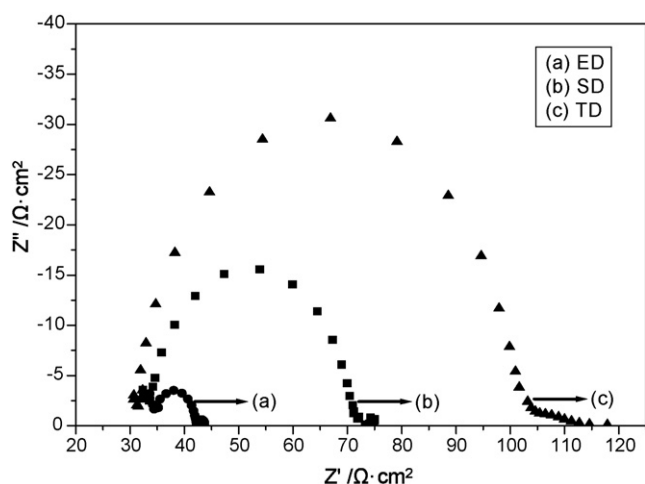


Fig. 6. Nyquist plots of the DSSCs fabricated with the Pt counter electrodes prepared by (a) electrochemical, (b) sputter, and (c) thermal depositions. The plots were recorded over a frequency range of 0.05–10<sup>5</sup> Hz, with an AC amplitude of 5 mV.

Pt counter electrode (ED cell) has shown a solar-to-electricity conversion efficiency of 7.6%, compared with 6.3% of the cell prepared with the TD-Pt counter electrode. The DSSC with the SD-Pt counter electrode has shown almost the same  $J_{sc}$  and conversion efficiency as those of a cell with the TD-Pt counter electrode. We observed that the  $J_{sc}$  and efficiency of the ED cell increased gradually with the electrodeposition time up to 900 s, and then remained at the same level up to 3600 s.

The dependence of  $J_{sc}$  on the Pt counter electrodes was further evidenced through electrochemical impedance spectroscopy. Fig. 6 compares resultant Nyquist plots of the DSSCs with the three counter electrodes. The semicircles represent the impedances related to charge transfer processes in the DSSCs. As the variable is only the Pt counter electrode, contributions to the impedance in virtue of the deposition methods are only taken into consideration. The plots suggest qualitatively that charge transfer resistance,  $R_{ct}$ , of a cell increases in the order of  $R_{ct}$  of ED-Pt film <  $R_{ct}$  of SD-Pt film <  $R_{ct}$  of TD-Pt film. The  $R_{ct}$  change in this study essentially refers to the component of resistance against electron transfer from the counter electrode to  $I_3^-$ , because other elements of resistances are common to all the DSSCs. A small  $R_{ct}$  indicates a facile electron transfer, whereas a large  $R_{ct}$  implies a sluggish electron transfer [22]. The smallest  $R_{ct}$  value of the ED-Pt cell correlates well with the highest  $J_{sc}$  value of the corresponding DSSC, which is attributable to the porous structure and increased surface area of the ED-Pt film. This less charge transfer resistance at the ED-Pt/electrolyte interface implies a more facile electron transfer from the counter electrode to  $I_3^-$  ions and thus an enhanced  $J_{sc}$  for the pertinent DSSC, compared with the  $J_{sc}$ s of the cells with the TD-Pt and SD-Pt counter electrodes. The increased fill factor of the DSSC with the ED-Pt electrode, compared with those of cells with TD-Pt and SD-Pt counter electrodes, also supports this observation. It is known that fill factor depends on the resistances of the photoanode, electrolyte, and counter electrode. Components of the resistances due to the photoanode and electrolyte being the same for the cells with the different Pt counter elec-

trodes, the difference in the fill factor in favor of the cell with the ED-Pt electrode should be due to its lower charge transfer and sheet resistances, relative to those of TD-Pt and SD-Pt counter electrodes.

It is generally accepted that the counter electrode should have good light reflecting characteristics to improve the light harvesting by the sensitizing dye [6,8], which in turn would additionally improve the  $J_{sc}$  of the pertinent DSSC. We measured light-reflecting properties of the three electrodes with TD, SD, and ED platinum layers. Table 1 shows the light reflectance values of the electrodes at the wavelengths of 488, 633, and 830 nm. It can be seen that the light reflectance of the ED-Pt film is far higher than those of TD-Pt and SD-Pt films in the visible and near IR region; this observation is qualitatively in consistency with the  $R_{rms}$  values of the Pt films. The increased light reflectance in the case of the ED-Pt counter electrode, relative to those of TD-Pt and SD-Pt counter electrodes, is advantageous for reducing the loss of the incident light due to transmittance, as evidenced by the higher  $J_{sc}$  in the case of the cell with the ED-Pt counter electrode.

In this study, we focused on the preparation of Pt counter electrodes by different deposition techniques and made a comparative investigation on the merits of such electrodes in terms of photovoltaic parameters of DSSCs. To facilitate this comparative investigation, we have not tried to improve the performance of the DSSCs, e.g., by incorporating a TiO<sub>2</sub> scattering layer, which would certainly enhance the efficiency of the DSSCs [23]. In each case of deposition of platinum film, viz. thermal, sputter and electrochemical depositions, we adopted their respective standard procedures, with the objective of obtaining the best possible efficiency for the DSSCs under our experimental conditions. We do not confirm the thickness of the platinum films to be exactly the same, though care was taken to obtain films of equal thickness. According to previous reports [2,3,24], thickness of the platinum film has insignificant influence on the performance of DSSCs and a 2 nm-thick Pt is sufficient to obtain a reasonable charge transfer resistance.

#### 4. Conclusions

Among the three counter electrodes prepared by depositing their Pt films by electrochemical, sputter and most commonly-employed thermal methods, the electrodeposited-Pt (ED-Pt) counter electrode has rendered a solar-to-electricity conversion efficiency of 7.6% for its DSSC, compared with approximately 6.4% of the cells prepared by using the other two types of counter electrodes. The sputter-deposited Pt film yielded almost the same photovoltaic characteristics as the thermal deposited Pt film. The improved performance of the DSSC with the ED-Pt counter electrode is attributed to the increased active surface area, decreased sheet resistance, and enhanced light reflection over the spectral range extending up to 830 nm of the ED-Pt film, with reference to the corresponding properties of the other Pt films. The improved catalytic activity of the ED-Pt film for the reduction reaction  $I_3^- + 2e^- \rightarrow 3I^-$  and the decreased charge transfer resistance at the counter electrode/electrolyte interface are correlated respectively with the increased active surface area and the decreased

sheet resistance of the ED-Pt film. The enhanced  $J_{sc}$  is also rationalized by the enhanced light reflection of the ED-Pt film, which facilitates improved light harvesting by the sensitizing dye.

### Acknowledgments

This work was supported by the Sol–Gel Innovation Project and the MOCIE new and renewable energy R&D project under contract 2006-N-PV12-P-05.

### References

- [1] K. Suzuki, M. Yamaguchi, M. Kumagai, S. Yanagida, *Chem. Lett.* 32 (2003) 28.
- [2] A. Hauch, A. Georg, *Electrochim. Acta* 46 (2001) 3457.
- [3] X. Fang, T. Ma, G. Guan, M. Akiyama, T. Kida, E. Abe, *J. Electroanal. Chem.* 570 (2004) 257.
- [4] K. Imoto, K. Takahashi, T. Yamaguchi, T. Komura, J.-I. Nakamura, K. Murata, *Sol. Energy Mater. Sol. Cells* 79 (2003) 459.
- [5] T. Hino, Y. Ogawa, N. Kuramoto, *Full Nanotubes Carb. Nanostruct.* 14 (2006) 607.
- [6] Z. Huang, X. Liu, K. Li, D. Li, Y. Luo, H. Li, W. Song, L. Chen, Q. Meng, *Electrochem. Commun.* 9 (2007) 596.
- [7] F. Cai, J. Chen, R. Xu, *Chem. Lett.* 35 (2006) 1266.
- [8] M.K. Nazeeruddin, A. Kay, I. Rodicio, R. Humphry-Baker, E. Müller, P. Liska, N. Vlachopoulos, M. Grätzel, *J. Am. Chem. Soc.* 115 (1993) 6382.
- [9] T.N. Murakami, S. Ito, Q. Wang, M.K. Nazeeruddin, T. Bessho, I. Cesar, P. Liska, R. Humphry-Baker, P. Comte, P. Péchy, M. Grätzel, *J. Electrochem. Soc.* 153 (2006) A2255.
- [10] Y. Saito, T. Kitamura, Y. Wada, S. Yanagida, *Chem. Lett.* 31 (2002) 1060.
- [11] M. Biancardo, K. West, F.C. Krebs, *J. Photochem. Photobiol. A: Chem.* 187 (2007) 395.
- [12] T. Ma, X. Fang, M. Akiyama, K. Inoue, H. Noma, E. Abe, *J. Electroanal. Chem.* 574 (2004) 77.
- [13] G. Wang, R. Lin, Y. Lin, X. Li, X. Zhou, X. Xiao, *Electrochim. Acta* 50 (2005) 5546.
- [14] N. Papageorgiou, W.F. Maier, M. Grätzel, *J. Electrochem. Soc.* 144 (1997) 876.
- [15] G.S. Attard, C.G. Göltner, J.M. Corcoran, S. Henke, R.H. Templer, *Angew. Chem. Int. Ed. Engl.* 36 (1997) 1315.
- [16] M.G. Kang, N.-G. Park, S.H. Chang, S.H. Choi, K.-J. Kim, *Bull. Korean Chem. Soc.* 23 (2002) 140.
- [17] P.A. Nelson, J.M. Elliott, G.S. Attard, J.R. Owen, *Chem. Mater.* 14 (2002) 524.
- [18] K.J. Hansen, C.W. Tobias, *J. Electrochem. Soc.* 134 (1987) 2204.
- [19] K.-S. Choi, E.W. McFarland, G.D. Stucky, *Adv. Mater.* 15 (2003) 2018.
- [20] N. Papageorgiou, P. Liska, A. Kay, M. Grätzel, *J. Electrochem. Soc.* 146 (1999) 898.
- [21] M. Matsumiya, W. Shin, N. Izu, N. Murayama, *Sens. Actuators B* 93 (2003) 309.
- [22] A.J. Bard, L.R. Faulkner, *Electrochemical Methods: Fundamentals and Applications*, John Wiley & Sons, New York, 1980, p. 350.
- [23] S. Hore, C. Vetter, R. Kern, H. Smit, A. Hirsch, *Sol. Energy Mater. Sol. Cells* 90 (2006) 1176.
- [24] X. Fang, T. Ma, G. Guan, M. Akiyama, E. Abe, *J. Photochem. Photobiol. A: Chem.* 164 (2004) 179.